

HIGH PRESSURE HYDROGEN JETS IN THE PRESENCE OF A SURFACE

Bénard, P.¹, Tchouvelev, A.², Hourri, A.¹, Chen, Z.², Angers, B.¹

¹ Hydrogen Research Institute, Université du Québec à Trois-Rivières, (P.O. Box 500),
Trois-Rivières, Québec, G9A 5H7, Canada, Pierre.Benard@uqtr.ca

² A.V. Tchouvelev & Associates Inc., 6591 Spinnaker Circle, Mississauga, Ontario, L5W 1R2,
Canada, atchouvelev@tchouvelev.org

ABSTRACT

The effect of surfaces on the extent of high pressure vertical and horizontal unignited jets is studied using CFD numerical simulations performed with FLACS Hydrogen, and Phoenix. For a constant flow rate release of hydrogen from a 284 bar storage unit through a 8.5 mm orifice located 1 meter from the ground, the maximum extent of the flammable cloud is determined as a function of time and compared to a free vertical hydrogen jet under identical release conditions. The results are compared to methane numerical simulations and to the predictions of the Birch correlations for the size of the flammable cloud. We find that the maximum extent of the flammable clouds of free jets obtained using CFD numerical simulations for both hydrogen and methane are in agreement with the Birch predictions. For hydrogen horizontal free jets there is strong buoyancy effect observed towards the end of the flammable cloud thus noticeably reducing its centreline extent. For methane horizontal free jets this effect is not observed. For methane, the presence of the ground results in a pronounced increase in the extent of the flammable cloud compared to a free jet. The effects of a surface on vertical jets are also studied.

1.0 INTRODUCTION

The properties of a high pressure jet originating from either a pressure relief valve or a small crack in the piping of a storage vessel depends on the leak location and size, the release conditions such as pressure and temperature and the physical properties of the gas such as velocity of sound, specific heat and molecular mass. High pressure jets will also be influenced by the presence of obstacles in the immediate surroundings, either impinging surfaces or turbulence inducing structures. From hydrogen safety considerations, interest lays in the determination of the extents of the flammable clouds which are very important parameters in the establishment separation distances and sizes of hazardous zones in the hydrogen codes and standards.

Birch *et al* [1] proposed a methodology to evaluate the decay of the mean concentration field along the centreline of a supercritical jet. The distance taken for the mean volume fraction concentration to decay to a given value in such flows is proportional to the diameter of the source and inversely proportional to the square root of the density of the jet fluid. In their analysis they showed that the concentration field behaves as if it were produced by a larger source than the actual nozzle source diameter; this is referred to as the pseudo-source. Later in 1987, Birch *et al* [2] reformulated their effective diameter definition based on the conservation of both mass and momentum. In a recent study, Houf *et al* [3] reused the Birch method to determine the concentration decay of unignited hydrogen jets. In their implementation, Houf *et al* reformulated the effective diameter of the pseudo-source by replacing the velocity at the end of the expansion region by an effective velocity originally

suggested by Hess *et al* [4] for under-expanded gas jets. They also removed the discharge coefficient in the effective diameter definition.

This study presents CFD simulations results of both free (i.e. unbound by a surface) and so-called wall (i.e. bound by a surface) horizontal and vertical jets using commercial software FLACS Hydrogen and Phoenics. Particular attention was given to the effects of proximity to the surface for horizontal and vertical hydrogen jet releases, which will impact the concentration decay. The results are compared to methane jets numerical simulations and to the predictions of the Birch correlations for the size of the flammable cloud.

2.0 BIRCH EFFECTIVE DIAMETER APPROACH AND THE MEAN CONCENTRATION DECAY

In the original implementation presented by Birch *et al* [1], the effective diameter d_{eff} is given by an expression of the form

$$d_{eff} = d \sqrt{C_d \frac{V_2 \rho_2}{V_3 \rho_3}}, \quad (1)$$

where d is the jet exit diameter, C_d is the discharge coefficient, V_2 and V_3 are the velocities of the gas at the exit of the reservoir and at the end of the expansion region respectively. Similarly ρ_2 and ρ_3 are the density of the gas at the exit and at the end of the expansion region. Birch *et al* made the hypothesis that $\rho_3 = \rho_g$, where ρ_g is the density of the gas at ambient conditions.

The velocity V_2 and the density ρ_2 are obtained from isentropic relations. The effective velocity at the end of the expansion region V_3 is given by an expression of the form

$$V_3 = \sqrt{\frac{\gamma T_3 R}{m_{mol}}}, \quad (2)$$

where γ is the specific heat ratio, T_3 is the temperature at the end of the expansion region, R is the universal gas constant and m_{mol} is the molecular weight.

The decay of the mean mole fraction $\bar{\eta}$ along the axis of a constant vertical jet can be expressed by

$$\bar{\eta} = \frac{K d_{eff}}{x + x_0} \sqrt{\frac{\rho_a}{\rho_g}}, \quad (3)$$

where K is the axial decay constant, d_{eff} is the effective diameter of the pseudo-source, x is the position along the centerline of the jet, x_0 is the virtual origin displacement of the jet, ρ_a is the density of air. The value of x_0 is generally neglected since $x \gg x_0$. The distance x_0 can also be approximated to be equal to 10% of d_{eff} . In their 1983 paper, Birch *et al* used a value of $K = 4.9$ based on experimental results obtained with natural gas, and a discharge coefficient value of $C_d = 0.85$ for the calculation of the effective diameter..

In the implementation by Houf *et al*, the following expression is used for the effective diameter d_{eff}

$$d_{eff} = d \sqrt{\frac{V_2 \rho_2}{V_3 \rho_3}}, \quad (4)$$

where it is assumed that $\rho_3 = \rho_g$. The velocity V_2 and the density ρ_2 are calculated using isentropic conditions. The effective velocity V_3 at the end of the expansion region is given by an expression of the form,

$$V_3 = V_2 + \frac{P_2 - P_3}{\rho_2 V_2}, \quad (5)$$

as originally suggested by Hess *et al* [4]. P_2 and P_3 are the pressure of the gas at the exit and at the end of the expansion region respectively. P_2 is calculated using isentropic relations. P_3 is assumed to be equal to the ambient pressure. Houf *et al* used the axial decay constant value $K = 5.4$ for hydrogen in the expression for the decay of the mean mole fraction in conformity with the correlation obtained by Birch *et al*.

3.0 DISPERSION SIMULATION RESULTS USING FLACS

A constant flow rate from an 8.48 mm diameter orifice of a 284.42 bar storage unit was studied numerically for both hydrogen and methane. The scenarios simulated here are:

- a) Horizontal and vertical free jets of hydrogen and methane
- b) Wall jets: In this case horizontal and vertical jets of hydrogen and methane are simulated in the presence of a surface. In all cases, the jets are located 1.024 m away from the surface.

The jet outlet conditions, i.e. the leak rate, temperature, effective leak area, velocity and the turbulence parameters (turbulence intensity and turbulent length scale) for the flow, are calculated using an imbedded jet program in FLACS. FLACS can also calculate the time dependent leak and turbulences parameters data for continuous jet releases in the case of high pressure vessel depressurization. The program is based on isentropic conditions and avoids simulating the supersonic region immediately downstream of the leak source by using a pseudo source approach. The procedure largely follows the Birch method in reference [2]. However, the reference condition in FLACS is modified to account for high velocities and air entrainment, while Birch *et al* used the stagnation reservoir condition. FLACS also includes the enthalpy equation and thereby makes the assumption of recovered temperature at the equivalent turbulent jet origin unnecessary. The conservation equation for mass, momentum, and enthalpy in addition to conservation equations for concentration, are solved on a structured grid using a finite volume method. The SIMPLE pressure-velocity correction method is used and extended for compressible flows with source terms for the compression work in the enthalpy equation. FLACS uses the k- ϵ turbulent model and the ideal gas equation of state.

For all the scenarios studied, the simulations were run as a function of time until steady-state was achieved, using a constant mass flow rate of 0.98618 kg/s for hydrogen and 2.7189 kg/s for methane.

The dimensions of the simulation domains and the number of cells are summarized for all the scenarios in tables 1-2.

Table 1. Dimensions of the simulation domains.

	Horizontal wall jet			Horizontal free jet			Vertical wall jet			Vertical free jet		
	x	y	Z	x	Y	Z	x	y	z	x	y	z
Dimension (m)	115	25	25	115	25	50	15	8.5	201	15	15	101

Table 2. Number of cells in each simulation domain.

	Horizontal wall jet	Horizontal free jet	Vertical wall jet	Vertical free jet
Hydrogen	171072	114048	435984	444672
Methane	57024			

3.1 Hydrogen jets simulation

Table 3 summarizes the results for the extent of the hydrogen jet at 4% molar fraction in air (LFL) for the different scenarios considered. For a horizontal wall jet, the maximum horizontal extent obtained was 52.5 meters at 13.7 sec. This maximum was achieved within the transient part of the release, while the steady state value obtained was 44.9 m, which was reached at 23.5 seconds after the beginning of the release. For a free jet, the maximum extent obtained was 35 m and only a very small transient maximum was observed.

For a vertical wall jet, a maximum transient length of 112.3 m was obtained at 48.8 seconds which eventually stabilized at 80 m after 85 seconds from the onset of the release. The extent of the free vertical jet was 42.4 m, in close agreement with the Birch/Houf *et al* result of 44.46 m.

Table 3. Computed extents of the hydrogen cloud contour at 4% molar fraction in air for the horizontal and vertical free and wall jets

Case studied	Extent at the jet centerline at steady state (± 0.5 m)	Maximal extent at steady state (± 0.5 m)	Maximal transient extent (± 0.5 m)	Time of maximal transient extent (± 0.2 s)	Time at which the jet become steady (± 0.2 s)
Horizontal wall jet	40.1	44.9	52.5	13.7	23.5
Horizontal free jet	22.8	35.0	36.5	10.1	20.0
Vertical wall jet	80.2	95.8	112.3	48.8	85.0
Vertical free jet	42.4		42.7	35.0	50.0

Figures 1-2 below show the contours of hydrogen at 4% molar fraction in air at steady state for the horizontal hydrogen free and wall jets.

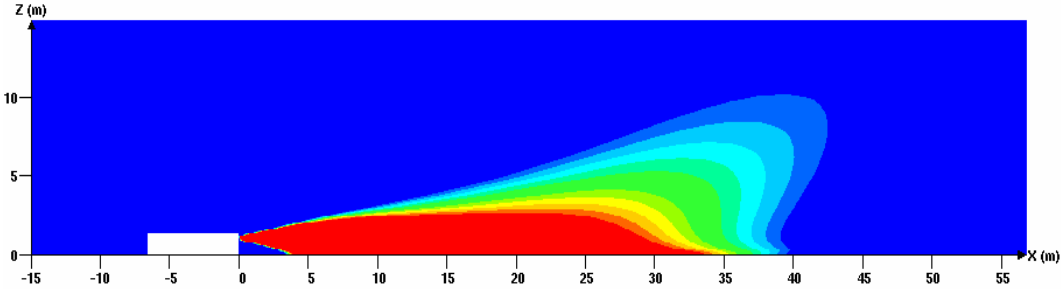


Figure 1. Contour of constant concentration (4% volume) of hydrogen in air at steady state for the horizontal wall jet (side view: longitudinal cut along the X-Z plane at Y=0.1 M)

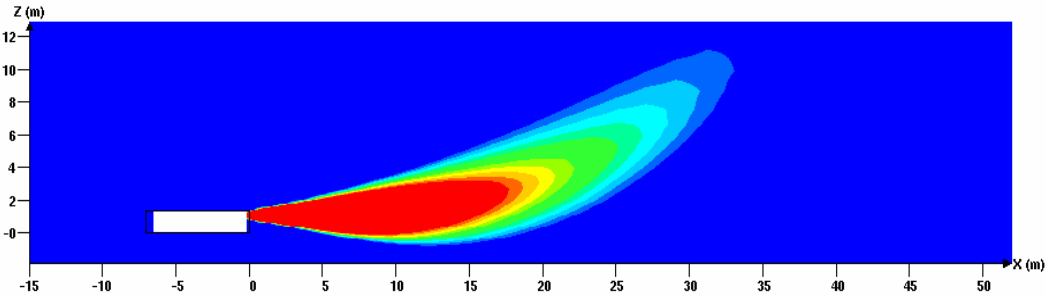


Figure 2. Contour of constant concentration (4% volume) of hydrogen in air at steady state for the horizontal free jet (side view: longitudinal cut along the X-Z plane at Y=0 m)

3.2 Methane jets simulation

Table 4 summarizes the extent of the methane cloud contour at 5% molar fraction in air (LFL) for the different scenarios simulated. The maximum extent of the flammable cloud at 5% (vol.) is reached at steady-state for all the scenarios studied except for the vertical wall jet. Similarly to hydrogen, Table 4 also shows that the presence of a surface in the proximity of the jet has an effect on the extent of the lower flammability contour. In this case, our results show a larger extent than that obtained for a free jets.

Table 4. Computed extents of the methane cloud contour at 5% molar fraction in air for the horizontal and vertical wall and free jets

Case studied	Extent at the jet centerline at steady state (± 0.5 m)	Maximal extent at steady state (± 0.5 m)	Maximal transient extent (± 0.5 m)	Time of maximal transient extent (± 0.2 s)	Time at which the jet become steady (± 0.2 s)

Horizontal wall jet	20.3	33.6	33.8	10.9	15.0
Horizontal free jet	14.7	14.9	14.9	6.1	6.1
Vertical wall jet	19.8	32.0	36.4	8.5	20.0
Vertical free jet	15.5		15.5	4.9	4.9

Figures 3-4 shows the contours of methane at 5% molar fraction in air at steady state for the horizontal methane free and wall jets.

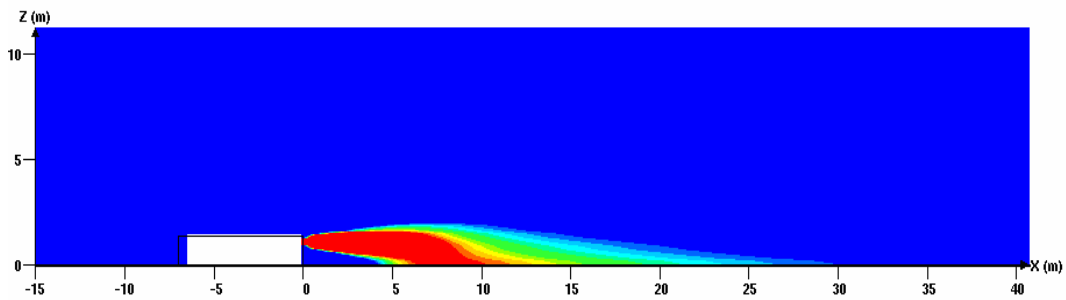


Figure 3. Contours of constant concentration (5% volume) of methane in air at steady state for the horizontal wall jet (Side view: longitudinal cut along X-Z plane at Y=0 m)

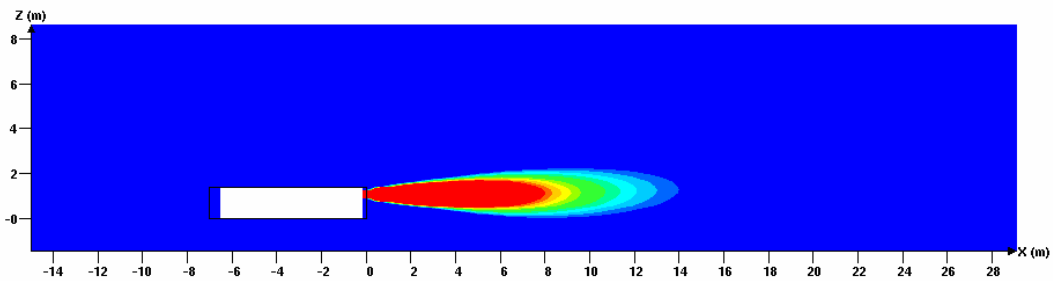


Figure 4. Contours of constant concentration (5% volume) of methane in air at steady state for the horizontal free jet (Side view: longitudinal cut along X-Z plane at Y=0 m)

4.0 DISPERSION SIMULATION RESULTS USING PHOENICS

4.1 CFD modeling of Birch experiments with natural gas

Birch's experiments on natural gas jets [1] were simulated with the commercial CFD software Phoenics using the properties of methane gas. Different symmetric domain sizes were used for the simulations. Figure 5 shows the volumetric concentrations obtained by the k-ε RNG and LVEL turbulence models for 3.5 bars. The LVEL turbulence model yields the simulation

results substantially deviating from the experiment data for high gas concentrations but shows good agreement with the experimental results around LFL concentrations. The k-e RNG model yields the results within 10% difference from the experimental for the whole range of concentrations. It can be seen that both CFD models reproduce the experimental data with acceptable accuracy at low concentrations around LFL (5% vol.). It has been validated before that k-e RNG produces very accurate CFD results for vertical free jets [5] while LVEL gives out acceptable and reliable results for description of far field concentrations in complex geometries and around surfaces [6]. The latter is of particular importance for high-pressure releases, where the use of LVEL model proved to be effective [7].

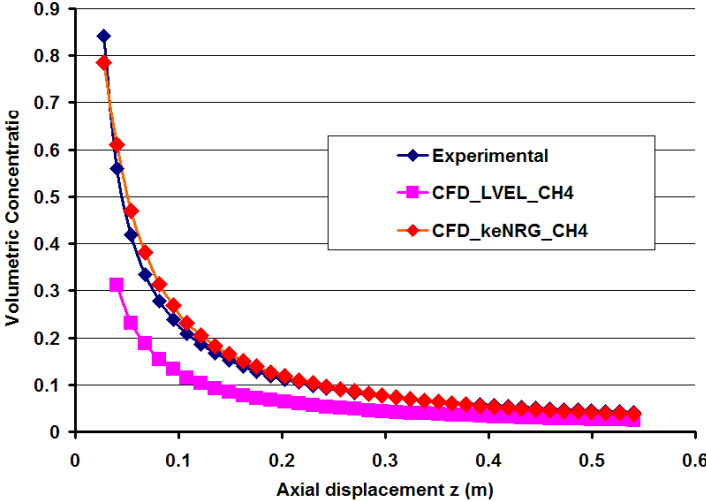


Figure 5. Comparison of CFD results with the experimental data from Birch et al [1] for a pressure of 3.5 bars.

Simulations were further performed for higher pressures (up to 170 bars) using the RNG k-ε model. The natural gas turbulent diffusivity is assumed to be 0.7 of turbulent viscosity, which is calculated by the kinetic energy and turbulent energy dissipation rate (k-e). Figure 6 shows the simulation data versus the experimental correlations for the pressures from 3.5 to 170 bars.

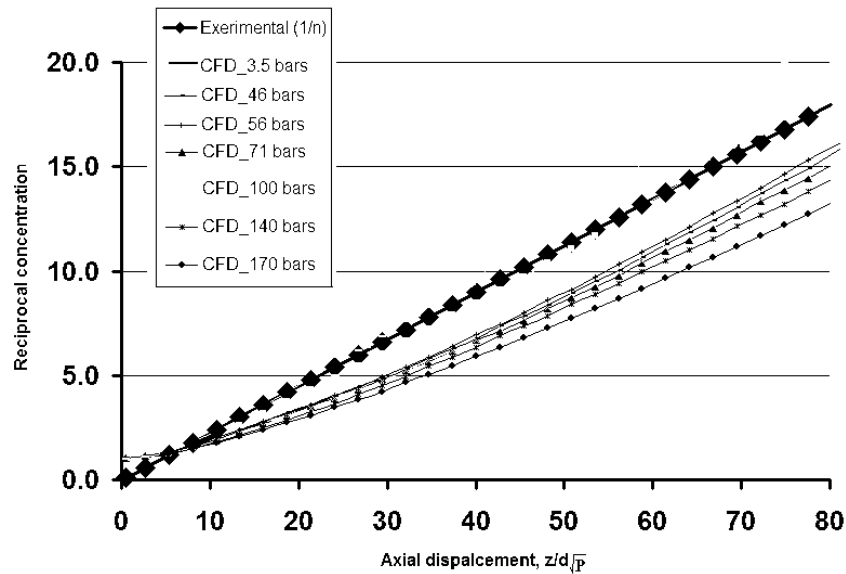


Figure 6. Comparison of CFD results with the experimental mean concentration for high pressure natural gas results showing collapse of the data in terms of $z/d\sqrt{P}$. Pressure range: 3.5 bars to 170 bars.

It can be seen that the numerical simulations reproduce the experimental data for various pressures with acceptable errors (within 20% for a wide range of pressures). It is interesting to note that simulations for pressures beyond the Birch range, i.e. >71 bars, produce greater errors. In general, the above trials confirm the validity of Birch correlations based on the experimental results for free vertical jets.

4.2 CFD modeling of hydrogen and methane wall jets

As specified above, both hydrogen and methane jet releases from storage tanks were simulated using a leak orifice of 8.48 mm ID and the stagnation pressure in the tank of 284.4 bars at 1 m above ground. It is estimated that the choked release lasts for 80 seconds for hydrogen and 240 seconds for methane. A symmetric domain of 100m long \times 8 m wide \times 25 m high was used to save computational resources and an optimal grid size of 40 \times 20 \times 30 was used to achieve accurate results with good convergence.

Figure 6 shows the comparison of LFL clouds caused by the hydrogen and methane releases with time using the real-gas law. The hydrogen release model was implemented by using the Abel-Noble real gas law and methane release was implemented using NIST real-gas properties. Note that Abel-Noble real gas law does not show consistency with methane under high pressure.









Time	Hydrogen	Methane
5 s	<p style="text-align: right;">Surface value 0.040000</p> 	<p style="text-align: right;">Surface value 0.050000</p> 
15 s	<p style="text-align: right;">Surface value 0.040000</p> 	<p style="text-align: right;">Surface value 0.050000</p> 
30 s	<p style="text-align: right;">Surface value 0.040000</p> 	<p style="text-align: right;">Surface value 0.050000</p> 
60 s	<p style="text-align: right;">Surface value 0.040000</p> 	<p style="text-align: right;">Surface value 0.050000</p> 

Figure 6. Comparison of transient hydrogen and methane jets using real gas law for both gases

Figures 7 and 8 show the transient hydrogen and methane cloud extents from the leak orifice for 60 and 90 seconds respectively. The buoyancy forces substantially shorten the LFL hydrogen cloud extent along the centreline extents in comparison with the maximum horizontal extent. This effect is not observed for methane. Also, at approximately 10 – 12 seconds from the onset of the release, both

gases experience a “puff” resulting in disconnect of a part of the cloud and its abrupt reduction in length. Figures 7 and 8 also show that the maximum extents of flammable clouds for both gases after the “puff” are close to each other (with the hydrogen one being a bit shorter). This is quite remarkable considering that the ratio of extents of hydrogen and methane free jets as shown in section 3.0 above and by Houf *et al* in [3] is approximately 3.5 to 1. This indicates that there is a significant effect of a surface on methane jet extent while it is quite weak for hydrogen.

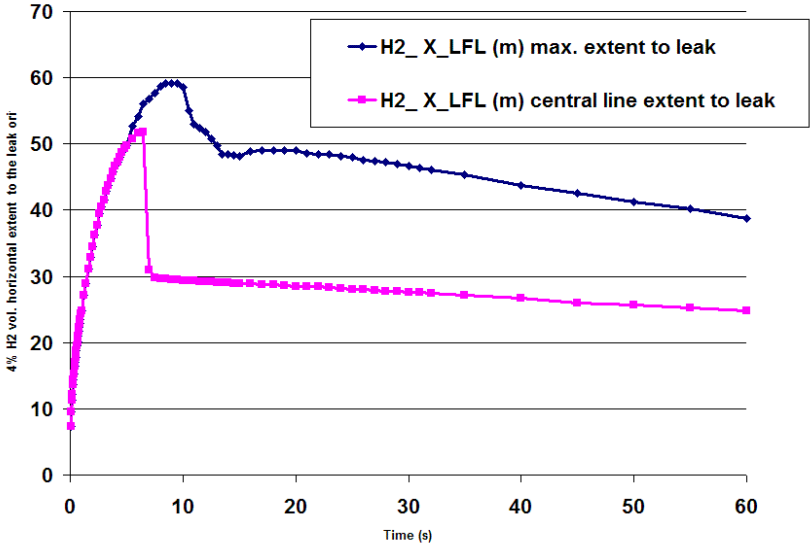


Figure 7. Hydrogen maximum and centerline cloud extents with time.

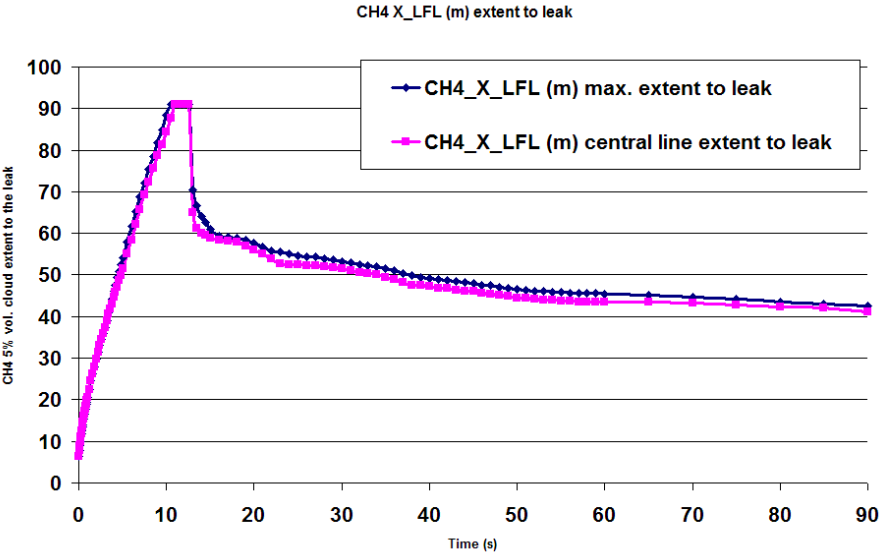


Figure 8. Methane maximum and centerline cloud extents with time.

5.0 DISCUSSION

Table 5 below shows the extent of the flammable envelopes using the Birch *et al* and Houf *et al* approaches for hydrogen and methane jets (respectively 4% and 5% molar fraction in air). Since both approaches were developed for vertical free jets, our simulation results for both hydrogen and methane free jets are within the range of the values predicted by Birch *et al* and Houf *et al*. For the sake of comparison, we included in the table, the computed values of the concentration decays for the free horizontal hydrogen and methane jets from our simulations results. This shows that the results for the horizontal free methane jets compare well with that of the vertical jets while those for hydrogen jets differ considerably.

Table 5. Comparison between the predictions made by Birch *et al* method and Houf *et al* method and FLACS simulations results for free hydrogen and methane jets

Gas	Birch et al. ($C_d=0.85$) (K=4.9)	Houf et al. (K=5.4)	Vertical free jet jet simulation (FLACS results)	Horizontal free jet simulation.(FLACS results)	
				Max. extent at steady state	Extent at the jet centerline at steady state
Hydrogen	46.35	44.46	42.4	35	22.8
Methane	13.21	12.32	15.5	14.9	14.7

For hydrogen horizontal free jets, the difference between the maximum extent at steady state and the centreline extent is attributed to the strong buoyancy effect observed towards the end of the flammable cloud, noticeably reducing its centreline extent. For methane horizontal free jets this effect is not observed. The presence of a surface for horizontal and vertical hydrogen and methane jets has a major impact on the flammable cloud extent at steady state. As shown in Table 6, the presence of a surface affected the the maximal extent of horizontal hydrogen jets, to a lesser extent (30% extent increase) than horizontal methane jets (125% extent increase) due to buoyancy. For vertical jets, the presence of a wall affected the maximal extent for both gases in practically the same way (113% increase for methane and 126% increase for hydrogen). Unlike hydrogen, the centerline extent of horizontal methane jets is smaller than the full extent because of a downward bending of the flammable envelope, which is a result of the contribution of the smaller buoyancy of methane compared to hydrogen (which reduces the rise of the jet as a function of distance with respect to hydrogen) combined with the reflection of the methane jet on the surface.

Table 6. Flammable cloud extent for horizontal and vertical hydrogen and methane wall jets. The values between brackets represent the extent values for corresponding free jets.

	Hydrogen (FLACS results)		Methane (FLACS results)	
	Extent at the jet centreline at steady state (m)	Maximal extent at steady state (m)	Extent at the jet centreline at steady state (m)	Maximal extent at steady state (m)
Horizontal wall jet	40.1 (22.8)	44.9 (35)	20.3 (14.7)	33.6 (14.9)
Vertical wall jet	80.2 (42.4)	95.8 (42.4)	19.8 (15.5)	32.0 (15.5)

Transient numerical simulations in Phoenics show that horizontal hydrogen and methane wall jets are affected by a horizontal surface in a dramatically different manner: hydrogen jet flammable extent behaves according to Birch / Houf predictions (about 45 m at 30 sec from the onset of the release – middle of the “steady state” plateau in Figure 7), while the extent of the flammable methane jet is significantly longer than predicted by Birch and Houf (about 45 m at 60 sec from the onset of the release – middle of the “steady state” plateau in Figure 8 – vs approximately 13 m for a free jet).

The above findings stress the importance of conducting further investigations of wall jets behaviour under the wide range of pressures and proximity to surfaces.

ACKNOWLEDGEMENTS

The authors would like to thank Natural Resources Canada (NRCan) and the Auto 21 Network of Centres of Excellence for their support and William Houf for useful discussions.

REFERENCES

1. Birch, A.D., Brown, D.R., Dodson, and Swaffield, The Structure and Concentration Decay of High Pressure Jets of Natural Gas, *Combustion Science and Technology*, **36**, 1984, pp. 249-261.
2. Birch, A.D., Hughes, D.J., and Swaffield, Velocity Decay of High Pressure Jets, *Combustion Science and Technology*, **52**, 1987, pp. 161-171.
3. Houf, W., Schefer, R., Predicting Heat Fluxes and Flammability Envelopes From Unintended Releases of Hydrogen, Proceedings of the 16th Annual Hydrogen Conference and Hydrogen Expo, March 31- April 1 2005, Washington DC, USA.
4. Hess, K., Leukel, W., and Stoeckel, A., Formation of Explosive Clouds ON Overhead Release and Preventive Measure, *Chemie-Ingenieur-Technik*, **45**, No 5, 1973.
5. Cheng, Z., Agranat, V.M. and Tchouvelev, A.V. Vertical Turbulent Buoyant Helium Jet – CFD Modeling and Validation. Proceedings of the 1st International Conference on Hydrogen Safety, Pisa, September 2005.
6. Agranat, V.M., Cheng. Z. And Tchouvelev, A.V., CFD Modeling of Hydrogen Releases and Dispersion in Hydrogen Energy Station. Proceedings of the 15th World Hydrogen Energy Conference, Yokohama, June 2004.
7. Tchouvelev, A.V., Cheng, Z., Agranat, V.M. and Zhubrin, S.V., Effectiveness of small barriers as means to reduce clearance distances. *International Journal for Hydrogen Energy*, 2006.